

# DESIGN STUDIES ON 100MeV/100kW ELECTRON LINAC FOR NSC KIPT NEUTRON SOURCE ON THE BASE OF SUBCRITICAL ASSEMBLY DRIVEN BY LINAC

Y. Chi, S. Pei, S. Wang, W. Liu, G. Pei, J. Cao, M. Hou, H. Song, Z. Zhou, R. Liu, C. Deng, X. Kong, G. Xu, X. Dai, J. Zhao, C. Ma, IHEP, P.R. China  
 M. Aizatskiy, I. Karnaukhov, V. Kushnir, V. Mytrochenko, A. Zelinsky, NSC KIPT, Kharkov, Ukraine

## Abstract

In NSC KIPT, Kharkov, Ukraine a neutron source based on a subcritical assembly and driven by a 100 MeV/100kW electron linac is under design and development. Design and construction of such a linac with high average beam current, low emittance and low beam losses are challenging tasks. In this paper the linac physical design with beam simulation results are described, the accelerating structures and some key technical solutions are presented.

## INTRODUCTION

In NSC KIPT, Kharkov, Ukraine a neutron source based on a subcritical assembly and driven by an electron linac is under design and development [1]. To provide a neutron flux of about  $10^{13}$  neutron/s it requires the linac with beam energy 100 MeV and beam power 100 kW. Design and construction of such a linac with high average beam current, low emittance and low beam losses are challenging tasks. Many key issues should be well solved, as follows.

- To cure the BBU effect due to high average beam current, several effective measures are adopted, such as using constant gradient structure to spread the HOMs frequencies in different cells, larger inner radius and shorter section length to have a higher group velocity as well as better shunt impedance by optimizing the structure geometry. In addition, the beam focusing with solenoids, triplets are used.
  - To avoid the beam loss in high energy region a chicane with a beam collimator, or a RF chopper located in low energy region will be employed to cut part of the beam with large energy spread caused in the beam bunching process.
  - To overcome the strong beam loading effect and to keep the beam energy spread to be small, a RF feed-forward compensation and a feedback control on the RF phase will be adopted.
  - To have a uniform electron density distribution on the target, a beam scanning method is considered with a set of correct magnet settings based on the beam emittance measurement.
- With the PARMELA [2] and MAD [3] simulations, the accelerator will provide beam emittance of  $5 \times 10^{-6}$  mrad, energy spread of 1%, and the beam particle losses rate for

the accelerated particles lower than 2%, and the beam density uniformity of better than 5% on the target are obtained. The main specifications of the linac are listed in Table 1.

Table 1: Main Specifications of KIPT Linac

Parameters	Unit	
RF frequency	2856	MHz
Energy	100	MeV
Beam current (max.)	0.6	A
Energy spread ( $1\sigma$ )	1	%
Emittance ( $1\sigma$ )	$5 \times 10^{-7}$	m-rad
Beam pulse length	2.7	$\mu$ s
RF pulse length	3	$\mu$ s
Pulse repetition rate	625	Hz
Klystron power	30/50	MW/ kW
Number of klystron	6	
Number of ACC. structure	10	
Length of ACC. structure	1.336	m
Gun voltage	$\sim 120$	kV
Gun beam current	2	A

## BEAM DYNAMICS

EGUN [4] and PARMELA [2] codes were used to simulate and optimize the linac design. Figure 1 shows the finalized linac layout. 6 klystrons and 10 accelerating sections are employed.

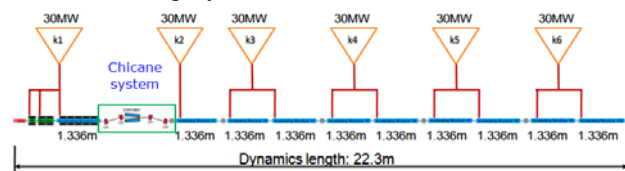


Figure 1: Schematic layout of the linac.

According to our simulation, there will be  $\sim 15\%$  particles at the downstream of the 1<sup>st</sup> accelerating structure which cannot meet the required 1% ( $1\sigma$ ) energy spread for 99% particles at the linac exit, and will be eliminated at the low energy stage by a chicane system shown in Fig. 2. The beam collimator is located between the 2<sup>nd</sup> and 3<sup>rd</sup> bending magnets to collimate the particles with large energy spread. Conclusively, the linac would have  $\sim 70\%$  transportation efficiency (from gun to linac exit). To get better beam performance, the chicane system was designed to be dispersion free at the system exit by optimizing the edge angles of CB2 and CB3 magnets.

About 2kW beam power will be lost in the collimator. As an alternative option, we may use a RF chopper system instead of the chicane system, which has a very attractive advantage that the beam collimation process can be done at very low beam energy of 120 keV. Finally, in order to get 0.60A electron beam at the linac exit, the maximum electron beam current at the gun exit should be  $\sim 0.85$  A for the chicane system option and  $\sim 1.8$ A for the RF Chopper one.

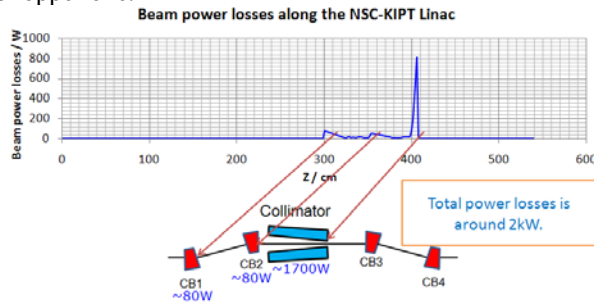


Figure 2: Beam power loss distribution along the linac.

The beam loss simulation is done with PARMELA [1]. Figure 2 shows the simulation result. Most of the beam power loss located at the chicane region, where the electron beam has relatively large energy spread and  $\sim 1.7$ kW beam power are collimated by the collimator. The total beam power loss along the whole linac (from electron gun to linac end) is  $\sim 2$ kW, about 2% of the total beam power at the linac exit.

Figure 3 shows the cumulative BBU effect calculation results. The left two plots are for no orbit correction cases, while the right two are for orbit correction cases. Here,  $+200\mu\text{m}/+200\mu\text{rad}$  initial beam offset and angle were assumed for the upper two plots, while  $+200\mu\text{m}/-200\mu\text{rad}$  for the lower two plots. If the largest beam offset is compared with the smallest aperture of the accelerating structure (23.726mm in diameter, see Table 2), it can be seen that the beam can successfully go through the linac by adopting better alignment with tolerance of less than 0.2 mm ( $1\sigma$ ) and beam orbit correction.

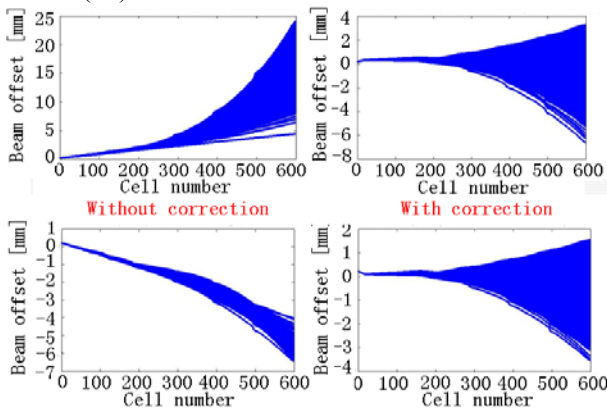


Figure 3: Beam offset distribution of one 0.85A (gun exit)/ $2.7\mu\text{s}$  beam along the whole linac.

The sketch of the transport line which transfers the beam from the linac exit to the target is shown in Figure 4. Two  $45^\circ$  vertical sector bending magnets, B1 and B2 are used

to rotate the beam from the linac to the target. A quadrupole (Q11) is placed at the middle point of the arc to cancel the dispersion. A triplet (Q6, Q7 and Q8) and another two quadrupoles (Q9, Q10) are used to form the beam size on the target. Because of the uncertainty of the beam twiss parameters at the Linac's exit, the triplet is also used for the emittance measurement together with the profile monitor PR3 by the quadrupole scanning method.

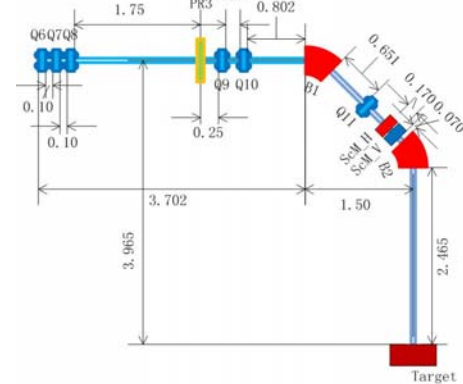


Figure 4: Layout of the transport line.

Beam scanning method is used to spread the beam pulses on the target evenly. According to beam repetition rate of 625 Hz, the scanning magnets (ScM\_H and ScM\_V) deflect these beam pulses to 625 different places in a second, which means there are 25 horizontal and 25 vertical scanning steps.

## MAIN COMPONENTS

The injector was designed and optimized to have better bunching efficiency and low energy spread as possible. It consists of a 120kV thermionic electron gun, a 2856MHz prebuncher, a 4-cell travelling wave buncher and a standard 1.336m travelling wave accelerating section. The linac would have  $\sim 70\%$  transportation efficiency from gun to linac exit.

10 accelerator structures are employed to boost the beam energy to 100MeV. Table 2 shows the accelerating structure main parameters.

Table 2: Accelerating Structure Parameters

Parameters		Unit
Operation frequency	2856	MHz
Operation temperature	$40.0 \pm 0.1$	$^\circ\text{C}$
Number of cells	34 +2 coupler cells	
Section length	1260 (36 cells)	mm
Phase advance per cell	$2\pi/3$ - mode	
Cell length	34.989783	mm
Disk thickness (t)	5.84	mm
Iris diameter (2a)	27.887 - 23.726	Mm
Cavity diameter (2b)	83.968 - 82.776	mm
Shunt impedance ( $r_0$ )	51.514 - 57.052	$\text{M}\Omega/\text{m}$
Q factor	13806 - 13753	
Group velocity ( $v_g/c$ )	0.02473 - 0.01415	
Filling time	215	ns
Attenuation parameter	0.1406	Neper

To suppress the BBU (both regenerative and cumulative) effects,  $\sim 1.3\text{m}$  long  $2\pi/3$  mode quasi-constant gradient structure was adopted. The disk whole diameter decreases from 27.887mm to 23.726mm in a stepwise fashion along the accelerating structure. To detune the dipole higher order modes quickly, dipole mode frequency spread was increased by increasing the average disk whole diameter step to  $\sim 0.122\text{mm}$ . At the 3<sup>rd</sup> to 6<sup>th</sup> disks of each accelerating structure, holes with diameter of 11mm will be drilled, by which the HEM11 mode frequency can be increased from  $\sim 4042\text{ MHz}$  to  $\sim 4050\text{ MHz}$ .

Due to the high averaged RF power loss in KIPT Linac structure, water jacket cooling is needed to sufficiently cool down the structure. With the High Frequency, Steady State Thermal and Structural solver modules in the multi-physics software package ANSYS, numerical RF-thermal-structural-RF coupled finite element analysis (FEA) on the NSC KIPT accelerating structure has been carried out. Finally, the cooling water flow rate is selected to be 10 t/hour.

The Linac consists of 6 klystron and its modulators. The 1<sup>st</sup> klystron energizes a prebuncher, a buncher and the 1<sup>st</sup> accelerating structure; The second klystron energizes the 2<sup>nd</sup> accelerating structure; each of the 3<sup>rd</sup> to 6<sup>th</sup> klystron energizes two accelerating structures respectively (see Fig. 1). About  $\sim 10\text{kW}$  and  $\sim 2\text{-}3\text{MW}$  input RF power are needed for the pre-buncher and buncher, 16MW and 20 MW power are needed for the 1<sup>st</sup> and 2<sup>nd</sup> accelerating structures (A0 and A1), 10MW input power is needed for each of the rest accelerating structures (A2-A9).

Linac LLRF system consists of one 2856 MHz signal generator, six controllers, six solid state amplifiers and some other related RF signal processing circuits. RF power stations 1-6 are connected to the LLRF system directly. The LLRF system can generate appropriate wave form for each RF station with amplitude and phase adjustable to compensate the beam loading effects and phase drift caused by various factors. The beam loading compensation is mainly based on feed forward control method and the phase drift based on feedback method.

The beam instrumentation system is capable to measure the beam performances such as beam positions, intensities, beam shape, emittance, beam loss, beam energy and energy spread, etc. Figure 5 shows the layout of the beam diagnostic components for the accelerator.

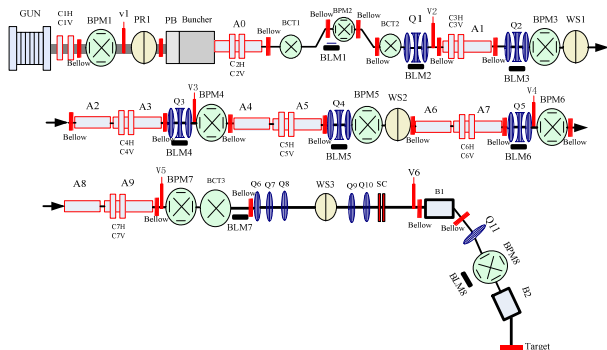


Figure 5: Beam Diagnostic Components.

The button type BPM will be used to measure the beam positions and angles, by which the beam trajectory can be determined. The beam shape measurement can provide additional information like emittance, beam energy and energy spread, based on the measurement of the beam size. The ACCT will be used to measure the beam current. The vacuum system will be divided to 7 sectors by 6 all metal gate valves. All metal gate valves are interlocked by the cold cathode gauges. The predominant pumps are diode-type and tri-type ion pumps. In the vacuum system, the range of working pressure is  $7 \times 10^{-7} \text{ - } 5 \times 10^{-5}\text{ Pa}$ . The quadrupole mass spectrometer will be used to monitor residual gas in the tube. Figure 6 shows the vacuum system layout for the linac.

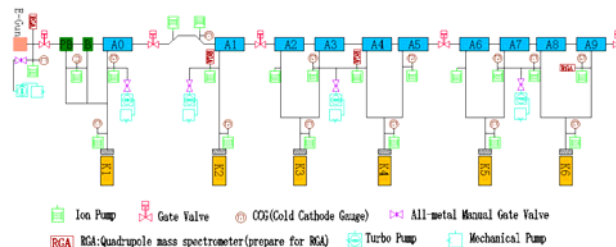


Figure 6: Vacuum system for NSC KIPT Linac.

The accelerator control system is based on EPICS to integrate and also use EPICS Channel-Archiver as KIPT accelerator’s data-base. Simens S7-200/300 PLC is selected as the system front-end I/O to control machine components such as magnet power supply and vacuum system. The timing system will adopt Event timing system, using the Micro-research EVG/EVR 230.

### SUMMARY

Most of the key issues for the design and construction on the KIPT-linac, such as BBU effects, beam loading effect, beam energy spread, beam emittance, and beam density uniformity on the target and so on, are briefly discussed. By solving these problems, the linac could meet the requirements as a driver of the neutron source. Further studies on these issues will be continuously done in the next steps of technical design, component fabrication and test, until the beam commissioning.

### REFERENCES

- [1] V. Azhazha, A. Dovbnya, I. Karnaukhov etc. “Project of a Neutron Source based on the Sub-critical Assembly Driven by Electron Linear Accelerator”, LINAC08, Victoria, Canada, September 29-October 3, 2008.
- [2] L. M. Young. PARMELA, Los Alamos National Laboratory, LA-UR-96-1835, Revised April22, 2003.
- [3] H. Grote and F. Schmidt. “MAD-X-an Upgrade from MAD 8”, PAC2003, Portland, USA, May 12-16, 2003.
- [4] W. B. Herrmannsfeldt. “EGUN – an electron optics and gun design program”, SLAC-331, 1988.